JOURNAL OF MATERIALS SCIENCE 29 (1994) 6592–6598

Crystallization and sinterability of cordierite-based glass powders containing CeO_2

B. H. KIM*, K. H. LEE†
* *Department of Materials Science and Engineering, Korea University, Seoul, Korea and*
† *Bio and Chemical Ceramics Dept, Ssangyong Research Center, Daejon, Korea*

Dense glass-ceramics for low firing temperature substrates were prepared by the addition of CeO_2 flux to a glass of the $MgO–Al_2O_3–SiO_2$ system. The glass powders were fabricated by melting at 1500 °C and ball milling. Glass powder compacts prepared by dry pressing were heated at 800–1000 °C for 0.5–4 h and sintered at 900–1000 °C for 3 h. The crystallization behaviour and sinterability of the glass powder compacts were analysed by thermal and thermomechanical techniques, X-ray diffractometry and scanning electron microscopy. The addition of CeO_2 prevents the formation of μ-cordierite phase in the glass-ceramics and improves the formation of α-cordierite phase. The activation energy of the glass containing CeO_2 for crystallization was lower than that of the CeO_2-free glass. Therefore, crystallization properties were enhanced. Because the crystallization onset temperature increased and the softening temperature decreased on the addition of CeO_2, the sinterability increased and dense glass-ceramics were fabricated below 1000 °C. The properties of the glass-ceramics containing CeO_2 appeared to be correct for low firing temperature substrates.

1. Introduction

In the past, alumina has been extensively used as substrate material because of its good thermal and mechanical properties [1–3]. However, its high sintering temperature (> 1500 °C) restricts the associated conductor materials to high-melting, costly and generally high-resistivity metals, and its high dielectric constant (~ 10) introduces significant signal propagation delay. Therefore, alternative materials, i.e. low firing temperature substrate with low sintering temperature (< 1000 °C), and low dielectric constant (~ 5), are required [4, 5].

Low sintering temperature enables copper-based conductor materials to be employed as substrates. If a copper-based conductor is used, it can fulfil the high signal propagation speed [6] and wiring density in electronic devices because copper has low resistivity. It is expected that a substrate having a low dielectric constant will also diminish signal propagation delay.

Cordierite-based glass-ceramics are attractive materials for preparing low firing temperature substrates due to this low dielectric constant (~ 5). It is difficult to obtain dense glass-ceramics below 1000 °C because the cordierite-based glasses ($MgO–Al_2O_3–SiO_2$) have high viscosity and narrow sintering temperature range [7, 8]. Because glass powder sintering proceeds by viscous flow [9], the decreasing glass viscosity shows good effect on its sinterability. In order to fabricate dense glass-ceramics, it may be a critical factor to select adequate flux which reduces glass viscosity. Components used as a flux should have a low activity and should not prevent crystallization. Because alkaline ions included in the substrate affect dielectric and electric properties, and react with conductor metals or solders, alkali oxides which are generally a good flux, cannot be used.

Zdaniewski [10] added CeO_2 and TiO_2 as a nucleating agent to the SiO_2-rich cordierite-based glass, and studied the effects of CeO_2 on bulk crystallization in bulk glasses. The effects of CeO_2 on surface crystallization in glass powders, however, has not been reported.

In this work, CeO_2 as a flux was added to a $MgO–Al_2O_3–SiO_2$ glass system in order to reduce the glass viscosity. It was reported that lanthanoid oxides generally reduce the viscosity of the glasses [11]. It is expected that a decrease in the glass viscosity should increase sinterability and enable the glass-ceramics to be synthesized below 1000 °C. If CeO_2 also shows good effects on surface crystallization properties, the glass-ceramics obtained can be applied as low firing temperature substrates for electronic devices.

This paper describes the new-surface crystallization behaviour and enhancement of sinterability resulting from the addition of CeO_2, and the properties of the glass-ceramics synthesized.

2. Experimental procedure

2.1. Glass preparation

The nominal composition of the starting glass (sample H5) was 20.2 MgO–24.4 Al_2O_3–49.4 SiO_2–5.0 TiO_2–1.0 B_2O_3 (wt %). CeO_2 was added to the starting glass in animals of 2, 5 and 10 wt %, and these com-

0022–2461

positions were named H5C2, H5C5 and H5C10, respectively.

The above mother glasses were melted in alumina crucibles using an electric furnace and quenched in a preheated furnace at 450 °C. Rods were prepared for thermomechanical tests. The glasses obtained were crushed in alumina-lined mills containing alumina balls and ethanol. The resulting slurries were dried, and then crushed to produce powders. The average particle size of the glass powders was in the range 3–4 μm.

2.2. Crystallization processes

In order to investigate the properties of the mother glasses, the true density of the glass powder (− 30 mesh) was determined using a gas pycnometer (Quantachrom Multipycnometer). Thermomechanical measurements were performed by a thermomechanical analyser (Rigaku, Model 811H, TMA unit) using quartz as a reference at a heating rate of 10 °C min^{-1}.

The formation of crystalline phases from the ground glass powders was followed using a differential thermal analyser at different heating rates (Rigaku, Model 811H, DTA unit).

Glass powders were biaxially pressed without binder in a 10 mm diameter steel mould at 220 MPa. These pellets were heated at 800–1000 °C for 0.5–4 h and crystalline phases were identified by X-ray diffractometry (Rigaku, D/Max-2A.) This was accomplished by quenching the samples from selected temperatures. They were crushed into fine powders and examined by nickel-filtered CuK_α ($\lambda = 0.15418$ nm) with 30 kV, 10 mA in the 2θ range from 7°–60° at a scanning rate of 4° min^{-1}.

The degree of crystallinity was determined by an internal standard method [12]. Crystallized samples were crushed and mixed with 30 wt % NaCl as a standard sample. They were examined using nickel-filtered CuK_α radiation with a present time of 4 s and step width of 0.01°.

Lattice parameters, a_0 and c_0, were obtained by Cohen's method [13] under the same conditions.

2.3. Measurement of sinterability

The shrinkage of the glass powder compacts was measured by TMA with a heating rate of 10 °C min^{-1}. Glass powders were biaxially pressed in a 5 mm diameter steel mould at 220 MPa.

Glass powders were biaxially pressed with a 8 × 30 mm steel mould at 1.7 ton cm^{-2} and sintered at 900–1000 °C for 3 h. Bulk and true density were measured by Archimedes' method and gas pycnometer, respectively, to obtain the relative density of the glass ceramics.

Microstructure studies on the glass-ceramics were performed by scanning electron microscopy (Jeol, JSM-35) with an accelerating voltage of 30 kV. The specimens were finely polished and etched by 1% HF solution for micrography.

2.4. Characterization

Dielectric measurements were made using a Gain Phase Analyser (Hewlett Packard, Model 4194A) at 1 MHz. Bending strength was measured using a Universal Testing Machine (Instron, Model 4204). The sample surfaces were polished up to 0.05 μm Al_2O_3 paste. The specimen dimensions were 1.5 mm × 2 mm × 25 mm. The thermal expansion coefficient was determined using Thermomechanical Analyser (Rigaku, Model 811H, TMA unit).

3. Results and discussion

3.1. Properties of glasses

CeO_2-free bulk glass (H5) was colourless and transparent. The yellow colour became deeper on increasing the amount of CeO_2.

As shown in Table I, the glass transition temperature, T_g, and softening temperature, T_s, decrease with increasing the CeO_2 content. It is assumed that cerium acts as a network modifier in the glass because it may have six or eight coordination numbers and its ionic field strength is 0.83 [14]. The sinterability of glasses with a low softening temperature can be enhanced because viscous flow occurs at lower temperature.

The density of the mother glasses increases with the amount of CeO_2 (Fig. 1). The increment of density for the glass containing 2 wt % CeO_2 is the largest. Densities of glasses having the same composition and different thermal history, can be compared with each other by assuming the magnitude of the interatomic bond strength. However, this cannot be applied to

TABLE I Glass transition temperature, T_g, and softening temperature, T_s, of mother glasses

Composition	T_g (°C)	T_s (°C)
H5	753	840
H5C2	745	814
H5C5	735	806
H5C10	734	801

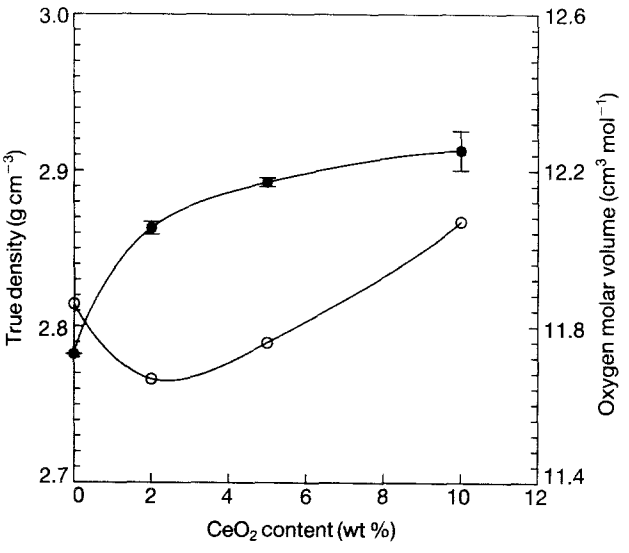

Figure 1 Effects of CeO_2 on (●) true density and (○) oxygen molar volume of mother glasses.

glasses of different compositions. In this study, an attempt has been made to compare the interatomic bond strength by calculating oxygen molar volume, V, because large oxygen ions almost occupy the total volume of the glass. Knowing the chemical composition of the glasses and their density, the oxygen molar volume can be calculated (Fig. 1). It decreases with the addition of 2 wt % CeO_2 but increases for the glasses containing 5 and 10 wt % CeO_2. Accordingly, it is considered that interatomic bond strength in the glass containing 2 wt % CeO_2 is the highest. Therefore, the large increment of true density for the glass containing 2 wt % CeO_2 may be attributed to both the large molecular weight of CeO_2 and the increment of interatomic bond strength.

The thermal expansion coefficient of the glass (Fig. 2) exhibits its minimum value at 2 wt % CeO_2 and increases with increasing amount of CeO_2. Generally, decreasing interatomic bond strength comes with decreasing T_g, decreasing T_s, increasing oxygen molar volume and increasing thermal expansion coefficient. In this study, the glasses containing 2–10 wt % CeO_2 show the above aspect. However, the glass containing 2 wt % CeO_2 has lower values of T_g, T_s, oxygen molar volume and thermal expansion coefficient than those of CeO_2-free glass. This may result from the change in the network structure of the glass. Crystallization properties may be changed by the addition of CeO_2 to the $MgO–Al_2O_3–SiO_2$ glass system.

The DTA thermograms of the glasses investigated are shown in Fig. 3. Some features of each thermogram are as follows:

(a) An endothermic peak signifying the glass transition temperature, T_g, is not present in all thermograms under the conditions of this experiment. This absence of an endothermic peak may result from the high activity of the fine glass powders.

(b) For the CeO_2-free glass (thermogram A) two exothermic peaks are present in the 895–970 °C temperature range. It was reported that μ-cordierite is formed preferentially and transformed to α-cordierite by further heating during crystallization of the $MgO–Al_2O_3–SiO_2$ glass. The first and second peak of thermogram A correspond to the formation of μ-cordierite and the transformation from μ- to α-cordierite, respectively. For the glasses containing CeO_2 (thermograms B, C and D) only one exothermic peak is present. The addition of CeO_2 apparently changes the crystallization process. This may result from a change of the glass structure by CeO_2.

(c) Both the crystallization onset temperature and the maximum point of the exothermic peaks shift slightly towards higher temperatures with increasing amount of CeO_2. These shifts may enhance sinterability because crystallization suppresses densification during glass powder sintering.

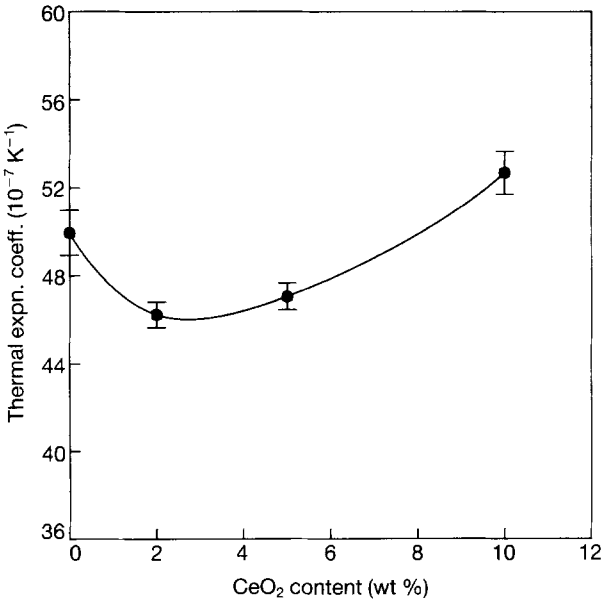

Figure 2 Effect of CeO_2 on thermal expansion coefficient of mother glasses.

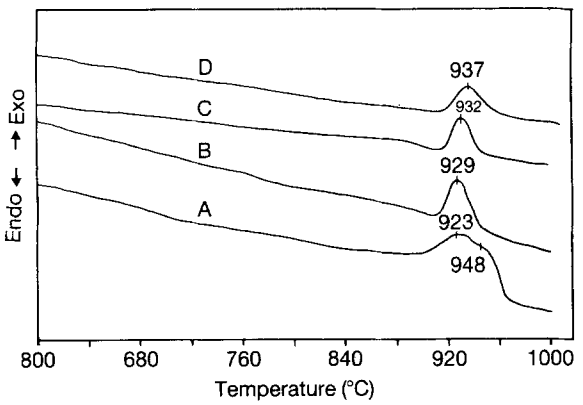

Figure 3 DTA curves of mother glasses at 10 °C min^{-1}: (A) H5, (B) H5C2, (C) H5C5 and (D) H5C10.

3.2. X-ray diffraction analysis (XRD)

Crystalline phases were identified after thermal treatment at 800–1000 °C for 0.5–4 h. The relative intensities and positions of the diffraction peaks agree with those assigned to μ- and α-cordierite (JCPDS card 27-716 and 13-293).

Observations of the XRD patterns are remarkable for samples heated at 850 and 900 °C for 1 h (Figs 4 and 5). Crystalline phases are well formed in the CeO_2-free sample heated at 850 °C (Fig. 4, A). But for the CeO_2 added samples heated at 850 °C (Fig. 4, B–D), the intensities of diffraction peaks are very weak, especially for the samples containing more than 5 wt % CeO_2 which hardly formed crystalline phases.

After the samples were heated at 900 °C, the XRD patterns of the CeO_2-free sample (Fig. 5, A) showed little difference from that heated at 850 °C. However, α-cordierite phase appears suddenly for the samples containing CeO_2 and the intensities of the diffraction peaks are very high (Fig. 5, B–D). A small amount of perrierite ($Ce_2Ti_2Si_2O_{11}$) is present as a minor phase in the samples containing more than 5 wt % CeO_2 when heated over 900 °C.

The transformation to the stable α-phase in the CeO_2-free sample occurs slowly and is completed when its sample is heated at 1000 °C for 3 h (Fig. 6). For the samples containing CeO_2, heated at

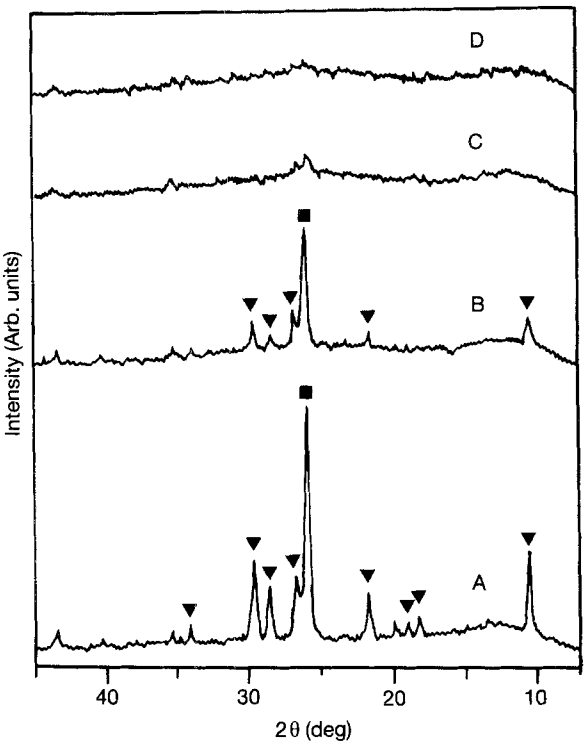

Figure 4 XRD patterns of the heat-treated glass at 850 °C for 1 h: (A) H5, (B) H5C2, (C) H5C5 and (D) H5C10, (▼) α-cordierite; (■) μ-cordierite.

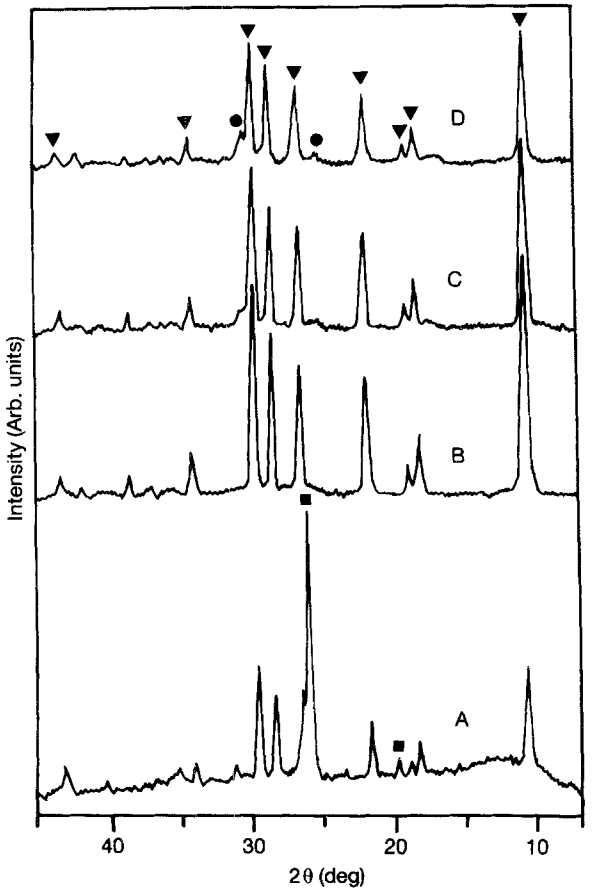

Figure 5 XRD patterns of the heat-treated glass at 900 °C for 1 h: (A) H5, (B) H5C2, (C) H5C5 and (D) H5C10, (▼) α-cordierite, (■) μ-cordierite, (●) perrierite ($Ce_2Ti_2Si_2O_{11}$).

900–1000 °C, the peak intensities are not widely different with varying soaking temperature and time. This means that the CeO_2-added glasses crystallized almost completely at 900 °C.

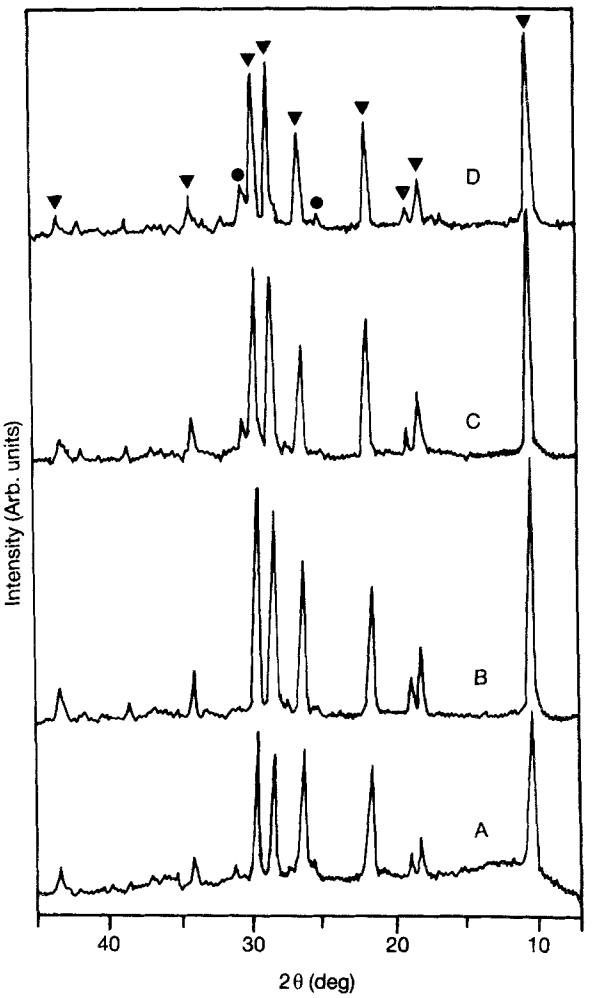

Figure 6 XRD patterns of the heat-treated glass at 1000 °C for 1 h: (A) H5, (B) H5C2, (C) H5C5 and (D) H5C10, (▼) α-cordierite, (●) perrierite ($Ce_2Ti_2Si_2O_{11}$).

The 2 wt % CeO_2 added sample shows the highest intensities of diffraction peaks and low background intensity in the 2θ range from 10°–20°. This is related to the degree of crystallinity (Table II). Integrated intensities were measured at α-cordierite (1 0 0) and NaCl (2 2 0) peaks. The degree of crystallinity, C, was calculated from the ratio of these integrated intensities

$$C = \frac{I_{cord}/I_{NaCl}}{(I_{cord}/I_{NaCl})\,100\%} \times 100 \qquad (1)$$

where I_{cord} and I_{NaCl} are the integrated intensities of the α-cordierite (1 0 0) peak and the NaCl (2 2 0) peak, respectively; the denominator represents the same ratio of integrated intensities in a fully crystallized sample. The samples heated at 1000 °C for 30 h were assumed to be crystallized completely and used as a fully crystallized sample.

The degree of crystallinity is very low for the CeO_2-free sample and shows a maximum at 2 wt % CeO_2. This is lowered slightly with the CeO_2 content. The value for the CeO_2-free sample heated at 900 and 950 °C for 3 h, is particularly low because these samples consist of α- and μ-cordierite phases and only α-cordierite was considered to determine the degree of crystallinity.

The diffraction peaks of these samples move slightly with increasing soaking temperatures and the amount

TABLE II Degree of crystallinity of glass-ceramics sintered at various temperatures for 3 h

Temperature (°C)	Degree of crystallinity (%)			
	H5	H5C2	H5C5	H5C10
900	30.1	84.1	80.0	80.0
950	36.6	95.0	88.5	85.0
1000	69.0	97.8	97.6	92.2

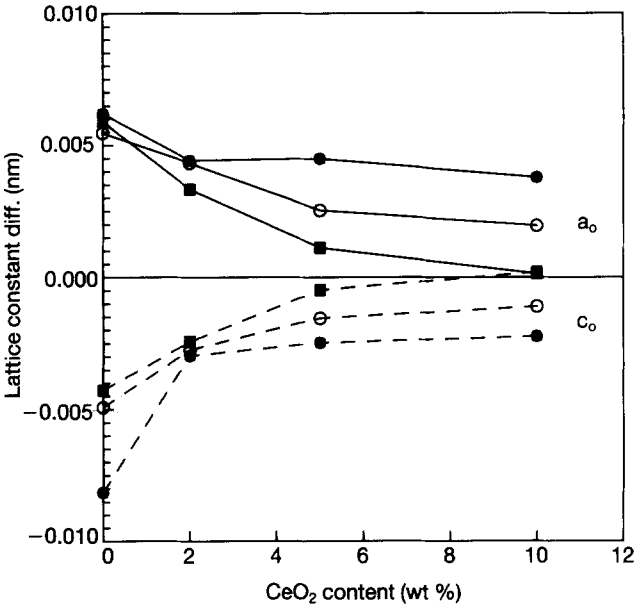

Figure 7 Lattice constant difference variations of the heat-treated glasses at (●) 900 °C, (○) 950 °C and (■) 1000 °C for (——) a_0 and (– – –) c_0: lattice constant difference = measured value-value in JCPDS card 13-193 (a_0 0.9770 nm; c_0 0.9352 nm).

TABLE III Crystallization temperatures (peak maximum) for mother glasses obtained at different heating rates

Heating rate (°C min^{-1})	T_c (°C)				
	H5[a]		H5C2	H5C5	H5C10
	1st	2nd			
2.5	894	909	897	900	908
5	908	916	913	915	918
10	923	948	929	932	937
20	952	971	950	952	958

[a] First and second peak maxima in the glass of H5 composition.

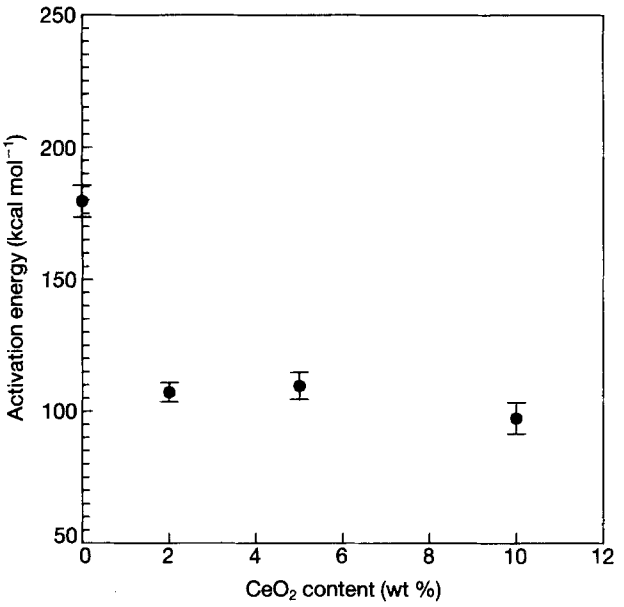

Figure 8 Effect of CeO_2 on activation energy of mother glasses for crystallization derived from the Kissinger equation: 1 cal = 4.1868 J.

of CeO_2 to higher or lower 2θ angles with the crystallographic directions. This indicates small changes in the structure of cordierite. Fig. 7 shows differences between measured lattice parameters and its value in JCPDS card 13-293 with temperatures and compositions. The lattice parameter comes closer to the value of JCPDS with increasing soaking temperatures and CeO_2 content.

As mentioned above, the addition of CeO_2 enhances crystallization properties of MgO–Al_2O_3–SiO_2 glass powder. In particular, it is suggested that 2 wt % CeO_2 is enough to elevate the crystallization properties.

3.3. Kinetics of crystallization

The activation energy for crystallization, E, of the glasses was calculated from the variation in the DTA peak temperature with heating rate. DTA results for the glass powders are listed in Table III. These results were fitted to the so-called Kissinger equation using the least square method [15]. When the crystallization process is assumed to be a first-order reaction, its expression is

$$\ln(a/T^2) = -(E/RT) + \text{constant} \quad (2)$$

where a is the heating rate (K min^{-1}) at which the DTA curves were recorded, T(K) is the maximum peak temperature of the crystallization exotherm, and E is the activation energy for crystallization (kcal mol^{-1}). Because the CeO_2-free sample showed two peak maxima in the DTA curve, the total activation energy for crystallization was obtained by summing both activation energies which were calculated for the first and second peaks, respectively. Fig. 8 shows the variation of activation energy for crystallization with the CeO_2 content. Its value is lowered over 60 kcal mol^{-1} by the addition of CeO_2, but does not vary with an increasing amount of CeO_2.

3.4. Sinterability

In order to investigate sinterability of the glass powder compacts, thermal shrinkage of these specimens was measured using a thermomechanical analyser (Fig. 9). The shrinkage increases with increasing temperature and the amount of CeO_2. The shrinkage of the sample containing 5 wt % CeO_2 is similar to that containing 10 wt % CeO_2 which is omitted because of overlap.

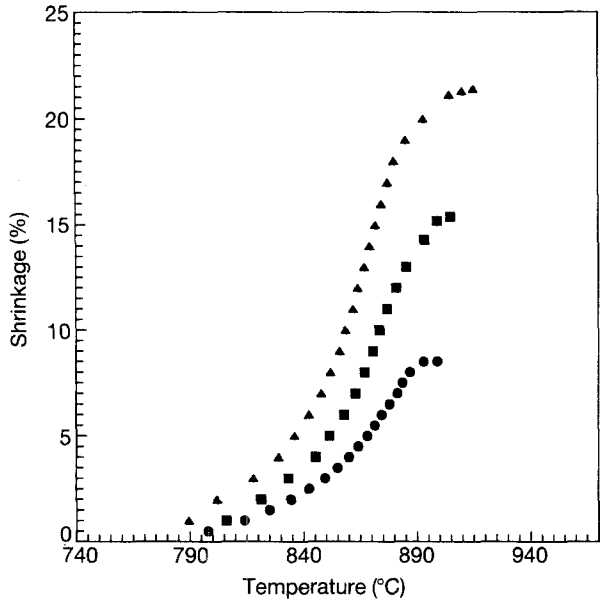

Figure 9 Shrinkage of glass powder compacts obtained by TMA at a heating rate of 10 °C min^{-1}: (●) H5, (■) H5C2 and (▲) H5C5.

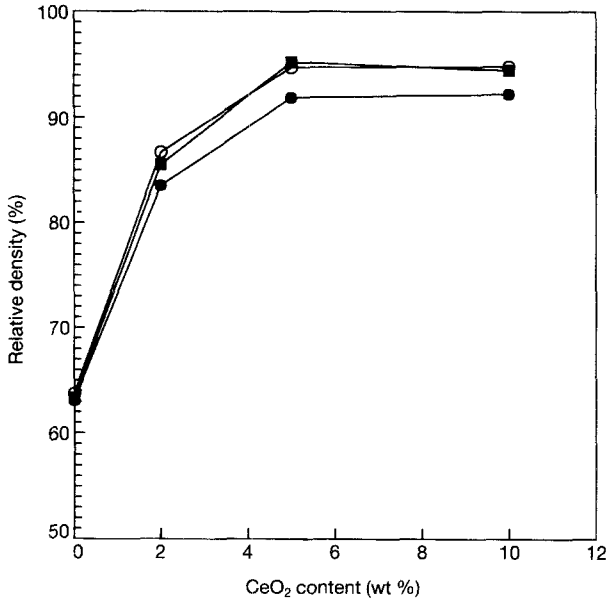

Figure 10 Relative density variations of glass-ceramics with CeO_2 content and soaking temperature sintered for 3 h at (●) 900 °C, (○) 950 °C and (■) 1000 °C.

Shrinkage ceases near each crystallization onset temperature of the glasses.

Fig. 10 shows relative densities of glass-ceramics sintered at 900–1000 °C for 3 h. Its value increases with soaking temperature and the amount of CeO_2. Enhanced sinterability may be attributed to the decrease in softening temperature and the increase of crystallization onset temperature by the addition of CeO_2. More than 5 wt % CeO_2 must be added for the purpose of enhancing sinterability.

Scanning electron micrographs (Fig. 11) were taken of a polished and etched section of glass-ceramic sintered at 1000 °C for 3 h. The sample containing 5 wt % CeO_2 (Fig. 11b) is dense and has a small amount of isolated pores. The CeO_2-free sample

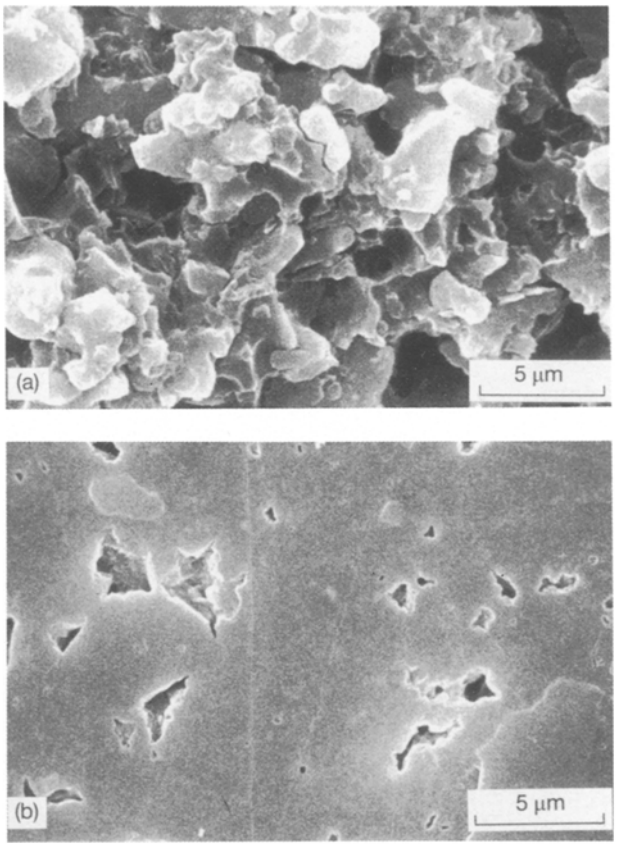

Figure 11 Scanning electron micrographs of polished and etched surface of glass-ceramics sintered at 1000 °C for 3 h: (a) H5 and (b) H5C5.

(Fig. 11a) is not densified as expected from the results of shrinkage and relative density.

3.5. Properties of glass-ceramics

Table IV gives the properties of the glass-ceramics sintered at 1000 °C for 3 h. All the glass-ceramics had effectively low dielectric constant although its value increased with the amount of CeO_2. Because the dielectric constant value is related to the porosity of the glass-ceramics, we corrected the measured value in order to investigate the compositional effect of CeO_2. The dielectric constant of air in the pores was assumed to be 1 and the rule of mixture was used. The measured and corrected dielectric constants are compared in Fig. 12. Area *A* gives the effect of porosity and area *B* that of the composition. As a result, it is considered that the dielectric constant was more dependent on the porosity of glass-ceramics than on the compositional variations resulting from the addition of CeO_2.

Bending strength showed its maximum at 5 wt % CeO_2. The good strength of the CeO_2-added glass-ceramics may be attributed to both good sinterability and the high degree of crystallinity. The 10 wt % CeO_2-added glass-ceramics yielded a lower value than that of the 5 wt % CeO_2-added sample. The cause of this is most probably due to the presence of perrierite.

For the CeO_2-added glass-ceramics, the thermal expansion coefficient and dissipation factor had favourable values for use as substrates.

TABLE IV Properties of glass-ceramics sintered at 1000 °C for 3 h

Properties	H5	H5C2	H5C5	H5C10
Bending strength (MPa)	80 ± 14	131 ± 8	178 ± 11	168 ± 12
Thermal expansion coefficient (10^{-7} K^{-1})	34.0	32.5	33.7	34.3
Dielectric constant (at 1 MHz)	3.6	4.6	4.9	5.4
Dissipation factor ($\times 10^{-3}$)	2.7	2.6	6.7	6.7

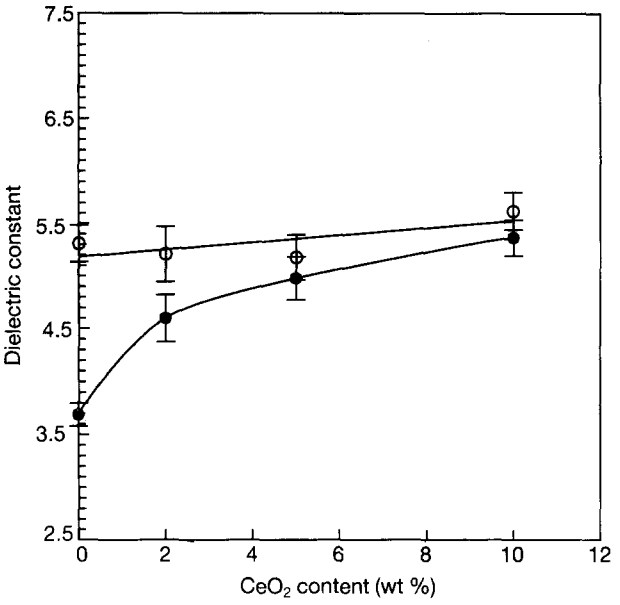

Figure 12 Dielectric constant variations of glass-ceramics with CeO_2 content sintered at 1000 °C for 3 h: (●) uncorrected, and (○) corrected with their porosity.

4. Conclusions

1. The addition of CeO_2 prevented the formation of μ-cordierite and improved that of α-cordierite. The activation energy of the glasses containing CeO_2 for crystallization was lower by more than 60 kcal mol^{-1} than that of the CeO_2-free glass. The degree of crystallinity increased with the addition of CeO_2.

2. The sinterability increased with increasing amount of CeO_2 because the softening temperature of the glass decreased and the crystallization onset temperature increased on the addition of CeO_2. Dense glass-ceramics were obtained from the glass powders containing CeO_2.

3. The glass-ceramics containing CeO_2 appeared to be suitable for low firing temperature substrates.

References

1. H. C. GRAHAM and N. M. TALLAN, in "Physics of Electronic Ceramics", edited by L. L. Hench and D. B. Dove (Marcel Dekker, New York, 1971) pp. 491–503.
2. J. M. HERBERT, in "Ceramic Dielectrics and Capacitors" (Gordon and Breach Science, Glasgow 1985) pp. 96–104.
3. B. SCHWARTZ, in "Electronic Ceramics", edited by L. M. Levinson (Marcel Dekker, New York, Basel, 1988) pp. 39–40.
4. R. R. TUMMALA, *J. Am. Ceram. Soc.* **74** (1991) 895.
5. K. KATA, Y. SHIMADA and H. TAKAMIZAWA, *IEEE Trans. Compos. Hybrids, Manuf. Technol.* **13** (1990) 448.
6. R. W. VEST, *Ceram. Bull.* **65** (1986) 631.
7. I. VEI, K. INOUE and M. FUKUI, *J. Ceram. Assoc. Jpn* **74** (1966) 27.
8. D. R. BRIDGE, D. HOLLAND and P. W. McMILLAN, *Glass Technol.* **26** (1985) 286.
9. T. J. CLARK and J. S. REED, *J. Am. Ceram. Soc.* **69** (1986) 837.
10. W. ZDANIEWSKI, *ibid.* **58** (1975) 163.
11. M. B. VOLF, in "Chemical Approach to Glass" (Elsevier, New York, 1984) pp. 391–405.
12. B. D. CULITY, in "Elements of X-ray Diffraction" (Addison-Wesley, London, 1978) pp. 415–17.
13. *Idem, ibid.*, pp. 363–8.
14. M. B. VOLF, in "Chemical Approach to Glass" (Elsevier, New York, 1984) pp. 63–4.
15. W. W. M. WENDLANDT, in "Thermal Methods of Analysis" (John Wiley, 1974) pp. 148–50.

Received 19 February 1993
and accepted 27 May 1994